Chemical Science

ROYAL SOCIETY OF CHEMISTRY

EDGE ARTICLE

View Article Online
View Journal | View Issue

Cite this: *Chem. Sci.*, 2024, **15**, 6141

All publication charges for this article have been paid for by the Royal Society of Chemistry

Received 8th January 2024
Accepted 17th March 2024

DOI: 10.1039/d4sc00128a

rsc.li/chemical-science

Temperature modulated sustainable on/off photosynthesis switching of microalgae towards hydrogen evolution†

Shangsong Li, Zhijun Xu, Song Lin, Luxuan Li, Yan Huang, Xin Qiao and Xin Huang *

Despite great progress in the active interfacing between various abiotic materials and living organisms, the development of a smart polymer matrix with modulated functionality of algae towards the application of green bioenergy is still rare. Herein, we design a thermally sensitive poly(*N*-isopropylacrylamide)-*co*-poly(butyl acrylate) with an LCST (*ca.* 25 °C) as a chassis, which could co-assemble with algal cells based on hydrophobic interaction to generate a new type of robust hybrid hydrogel living material. By modulating the temperature to 30 °C, the volume of the polymer matrix is shrunk by 9 times, which allows the formation of physical shading and metabolism changing of the algae, and then triggers the functionality switching of the algae from photosynthetic oxygen production to hydrogen production. By contrast, by decreasing the temperature to 20 °C, the hybrid living materials go into a sol state where the algae behave normally with photosynthetic oxygen production. In particular, due to the proliferation of the algae in living materials, a long-term and exponential enhancement in the amount of hydrogen produced is achieved. Overall, it is anticipated that our investigations could provide a new paradigm for the development of polymer/living organism-based hybrid living materials with synergistic functionality boosting green biomanufacturing.

Introduction

Natural photosynthesis plays a key role in the development of green solar energy storage technologies. The solar energy that the Earth is exposed to in 1 minute exceeds the human world-wide energy demand for 1 day.[1] But the attempt to directly utilize nature in the form of non-fossilized biofuels poses its own set of challenges, since most photosynthetic organisms prioritize the optimization of survival strategies rather than solar-to-bioenergy conversion efficiency. For example, the solar–biomass conversion efficiencies of photosynthetic organisms are within the range of only 0.2–8%.[2] Since the same photosynthetic system is used, which results in a sluggish photoelectron supply towards hydrogenase at the reducing end of the photosynthetic chain, this remains a considerable challenge to desirable photohydrogen production. In this regard, besides biotechnological strategies,[3–6] the recently developed technique of combining abiotic substances with living organisms has also been recognized as a feasible pathway for boosting photohydrogen production from solar energy,[7–13] which should then offer promising opportunities to solve the energy crisis and concurrent environmental problems. By taking algae as an example, various abiotic materials, including silicon dioxide,[14,15] gelatinizable protein,[16] catalytic enzyme,[17,18] conductive polymer and photosensitive nanoparticles,[19,20] have been successfully incorporated either onto the surface of or inside the algal cell,[21,22] and then the integrated materials could facilitate the generation of a mild hypoxic microenvironment, enabling the activation of intracellular hydrogenase to induce the functionality switching of algal cells from normal oxygen evolution to photosynthetic hydrogen production. For example, by forming a sandwich-like layer around a single algal cell, laccase-catalyzed oxygen-consuming reaction triggered hydrogen production was achieved at the rate of 0.32 μmol H_2 per h per mg chlorophyll for 7 days.[17] Alternatively, by combining *in situ* interfacial polymerization and biomineralization, a cellular bionic system based on combining algal cells with a conductive PPy/$CaCO_3$ hybrid shell was constructed where the added photosensitizer was capable of generating and transferring exogenous electrons into photosynthesis-associated metabolisms, which augmented photosynthetic efficiency and orchestrated photosynthetic pathways to provide more photoelectrons across the photosynthetic chain for enhanced hydrogen evolution.[20] Despite the above developments, during the formation of an anaerobic microenvironment for photobiological hydrogen production, a host of high-value substances, including glucose[23,24] and enzymes[17,18] as well as electron sacrificial agents[20,25] are widely

MIIT Key Laboratory of Critical Materials Technology for New Energy Conversion and Storage, School of Chemistry and Chemical Engineering, Harbin Institute of Technology, China. E-mail: xinhuang@hit.edu.cn

† Electronic supplementary information (ESI) available. See DOI: https://doi.org/10.1039/d4sc00128a

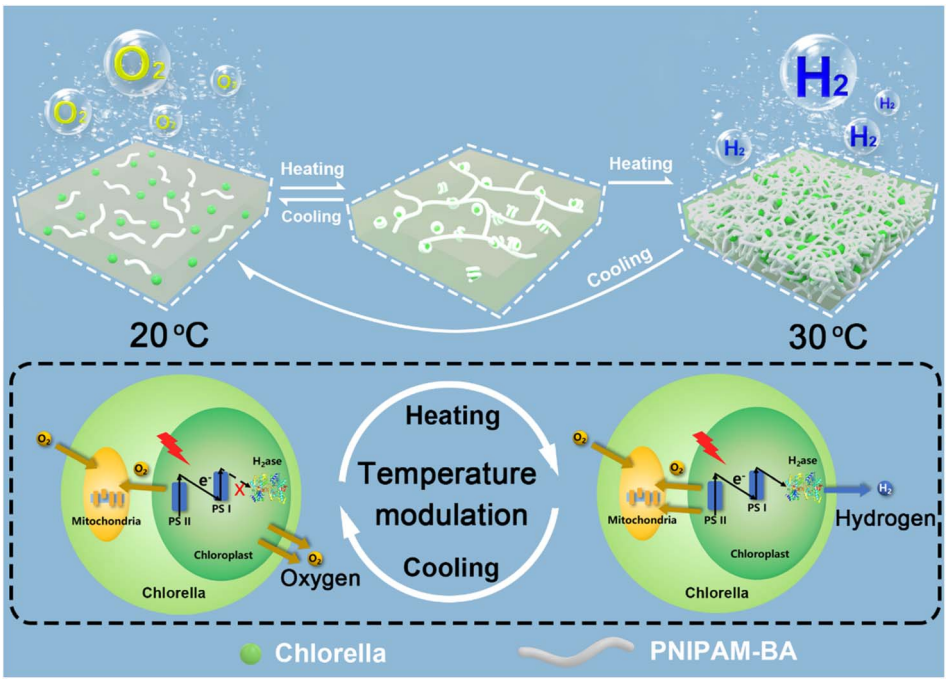

Scheme 1 Schematic illustration showing the programmed modulation of hydrogen and oxygen evolution based on the reversible sol–gel switching of the constructed polymer–*Chlorella* living material.

utilized, limiting the sustainability of the systems. Moreover, currently, most of the constructions obtained by combining an abiotic substance and living cells focus on the linear superposition of living cell functions and abiotic functions.[26–28] There are few reports on the synergistic effect of living cells and abiotic matrices conferring advanced functionalities on living cells, such as on-demand reversible on/off modulation of biological hydrogen production by algal cells, which is also a challenge and bottleneck for future advances in photobiological hydrogen production.[29–31]

Green algae, as an environmentally friendly third-generation biofuel, can directly use inexhaustible resources: sunlight energy and substrate water, to generate renewable and carbon-neutral biohydrogen, which it is anticipated will then contribute to solving the environmental pollution and energy-demand problems associated with fossil fuels.[18,32] Herein, we choose *Chlorella pyrenoidosa* (a type of green algae) as a building block to generate a new type of sustainable photohydrogen production system with on-demand functionality switching. In particular, by incorporating a hydrophobic monomer butyl acrylate into a temperature-sensitive poly(*N*-isopropylacrylamide), the obtained poly(*N*-isopropylacrylamide)-*co*-poly(butyl acrylate) (PNIPAM-*co*-BA) could efficiently co-assemble with *Chlorella* cells to form a type of polymer–*Chlorella* based hydrogel living material. We demonstrate that the *Chlorella* cells in the PNIPAM-*co*-BA sol-state matrix could achieve physiological activities which are consistent with the natural state, such as photosynthesis, oxygen production and proliferation. Whereas, when the sol matrix is switched to a gel matrix, the shading effect on *Chlorella* caused by the volume shrinkage of PNIPAM-*co*-BA increases, and then the photosynthetic oxygen production rate of *Chlorella* decreases,[33] which helps the *Chlorella* in the living material to establish an anaerobic balance between photosynthetic oxygen production and respiration oxygen consumption.[17] The activity of hydrogenases within the *Chlorella* is then activated,[18] causing the living material to switch from photosynthetic oxygen production to hydrogen production on demand (Scheme 1). Clearly, the long-term viability of the green algae inside the polymer matrix without the addition of other high-value chemicals make a significant contribution to the enhancement of sustainability, and the easy temperature-based modulation of photohydrogen production should also allow the possibility of implementing macroscopic-level photohydrogen production in the future.

Results and discussion

Construction of PNIPAM-*co*-BA/*Chlorella* hybrid hydrogel living material

Given the inactivity of the native *Chlorella* cell wall, which is made up of cellulose, hemicellulose, pectin and protein,[28,34] a hydrophobic alkyl-chain-containing monomer (butyl acrylate) is specially incorporated into the thermally sensitive PNIPAM to generate a hydrophobic interaction with native *Chlorella*. Meanwhile with the incorporation of butyl acrylate into PNIPAM, the lower critical solution temperature (LCST) of the copolymer decreases. In this study, 5 wt% of PNIPAM-*co*-BA (Fig. S1†) was specially used, which showed an LCST of *ca.* 25 °C upon heating of 0.1 wt% copolymer in BG-11 medium (Fig. S2 and S3†). Also, the synthesized PNIPAM-*co*-BA exhibited a transparent low-viscosity (0.0025 Pa s) sol state at 20 °C without compromising the normal photosynthesis of *Chlorella* (Fig. S4, S6† and 3g), and by contrast could show a non-transparent gel state by increasing

the temperature above the LCST at 30 °C (Fig. S6†). Accordingly, by taking advantage of such a copolymer as a matrix, after mixing with *Chlorella* at 20 °C (Fig. S6†), a polymer–*Chlorella* hybrid homogeneous solution—a sol-state living material (SSLM)—was formed with low viscosity (0.0016 Pa s) (Fig. S4†). Whereas, by heating the solution above the LCST to 30 °C, a polymer–*Chlorella* gel-state living material (GSLM) formed immediately (Fig. S5†). After incubation for 2 hours at 30 °C, it exhibited robust and elastic properties (Fig. S6†). It was observed that various shapes of living materials, including flower, square, heart, circle and hexagon, could be obtained at large scale with good dispersion of *Chlorella* inside the polymer matrix (Fig. 1a, b, S7 and Video S1†).

Significantly, the whole formation procedure showed good biocompatibility. In this study, by using a copolymer (5 wt%) and a *Chlorella* suspension (7.55×10^7 cells per mL) to generate living material (Fig. S8†), the viability of *Chlorella* in the living material recorded within 24 hours could be as high as 98.6% (Fig. S9 and S10†). Moreover, even the living material in the gel state, due to it containing 40 wt% water (Fig. 1c), can well maintain the normal physiological activities of *Chlorella*. Within 7 days, there was no significant difference in the survival ratio between the *Chlorella* in living material and the control group: both were above 90% (Fig. S11 to 16† and 1d). But it should be mentioned that, if the concentration of the copolymer is increased further to 7.5 wt% or 10 wt%, the osmotic pressure arising from PNIPAM-*co*-BA leads to an obvious decrease in the survival ratio of *Chlorella* (Fig. S9 and 10†).

Moreover, due to the physical crosslinking role of *Chlorella* inside the polymer matrix, the formed living material in the gel state demonstrates good mechanical properties. In this study, by using 7.55×10^7 cells per mL of *Chlorella* and 5 wt% of PNIPAM-*co*-BA to generate the hydrogel living material, its elastic modulus could reach as high as 4.59 MPa (Fig. 1e and S21†), comparable to the performance of engineered polyurethane foam ranging from 2.15 to 3.63 MPa.[35] As shown in the details of oscillatory shear experiments, when the living material was in the gel state, at < 0.05% strain, a linear viscoelastic response from the living material was observed. At this time, the storage modulus G' was larger than the loss modulus G'', and both G' and G'' were independent of strain, which was characteristic of the elastic response of the gel network. At > 0.1% strain, the living material exhibited nonlinear viscoelastic behavior, and beyond the yield strain, the disruption of the physically crosslinked network caused both G' and G'' to decrease along with the increased strain (Fig. S17†). Similarly, when the living material was in the sol state, G' between 0.86 and 1.36 Pa, and G'' between 0.09 and 0.38 Pa were observed (Fig. S20†).

At temperatures above the LCST, we attribute to the hydrophobic interaction between *Chlorella* and the copolymer a key role in the formation of the robust living material. To confirm this, the copolymer was labelled with a green fluorescence dye (fluorescein *O*-methacrylate), and the confocal fluorescence images clearly show the appearance of green fluorescence around the algal spheroids at 30 °C (Fig. 2a–c), where the *in situ*

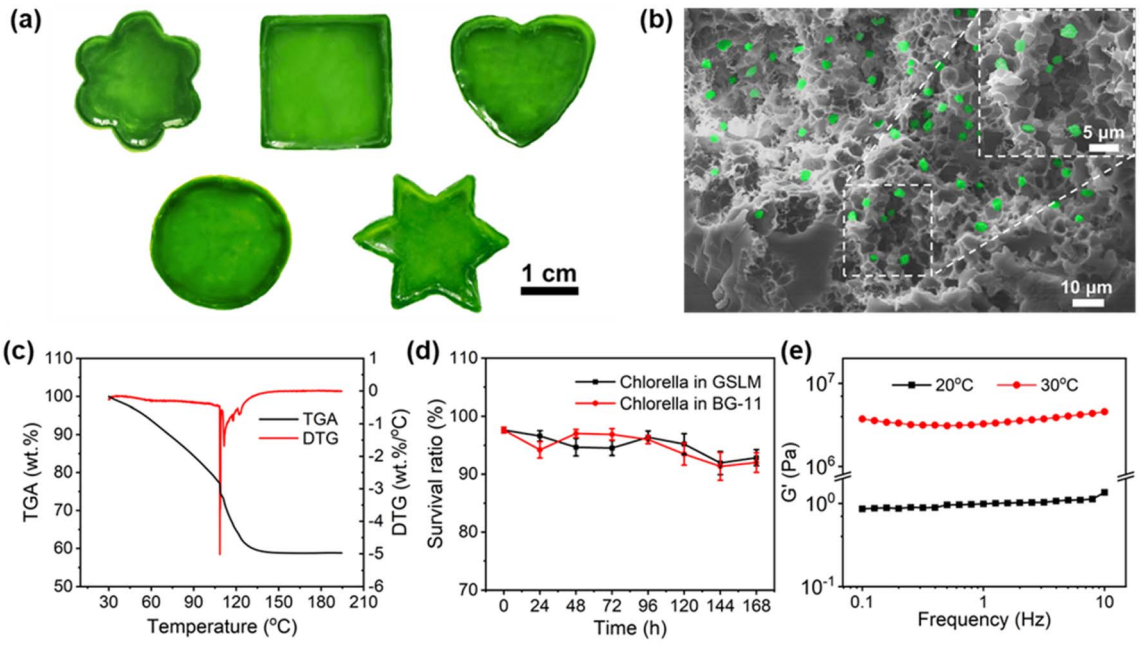

Fig. 1 Construction and characterization of polymer–*Chlorella* living material. (a) Gel-state living material (GSLM) of different shapes (flower, square, heart, circle, hexagon) prepared from modeled sol-state living material (SSLM). Scale bar, 1 cm. (b) Pseudo-colored SEM image of GSLM formed from PNIPAM-*co*-BA and *Chlorella* at 30 °C for 2 hours. Scale bar, 10 μm. Inset shows a partially magnified pseudo-colored SEM image. Scale bar, 5 μm. (c) Thermogravimetric analysis (TG) and derivative TG (DTG) curves of GSLM. (d) *Chlorella* survival ratio in GSLM (black squares) and BG-11 solution (red circles) for 7 days ($n = 3$, mean ± SD). The *Chlorella* survival ratio was calculated by dividing the number of green fluorescent *Chlorella* by the number of red fluorescent *Chlorella*. (e) Variation in storage modulus of SSLM and GSLM with *Chlorella* concentration of 7.55×10^7 cells per mL and PNIPAM-*co*-BA concentration of 5 wt% at 20 °C (black squares) and 30 °C (red circles).

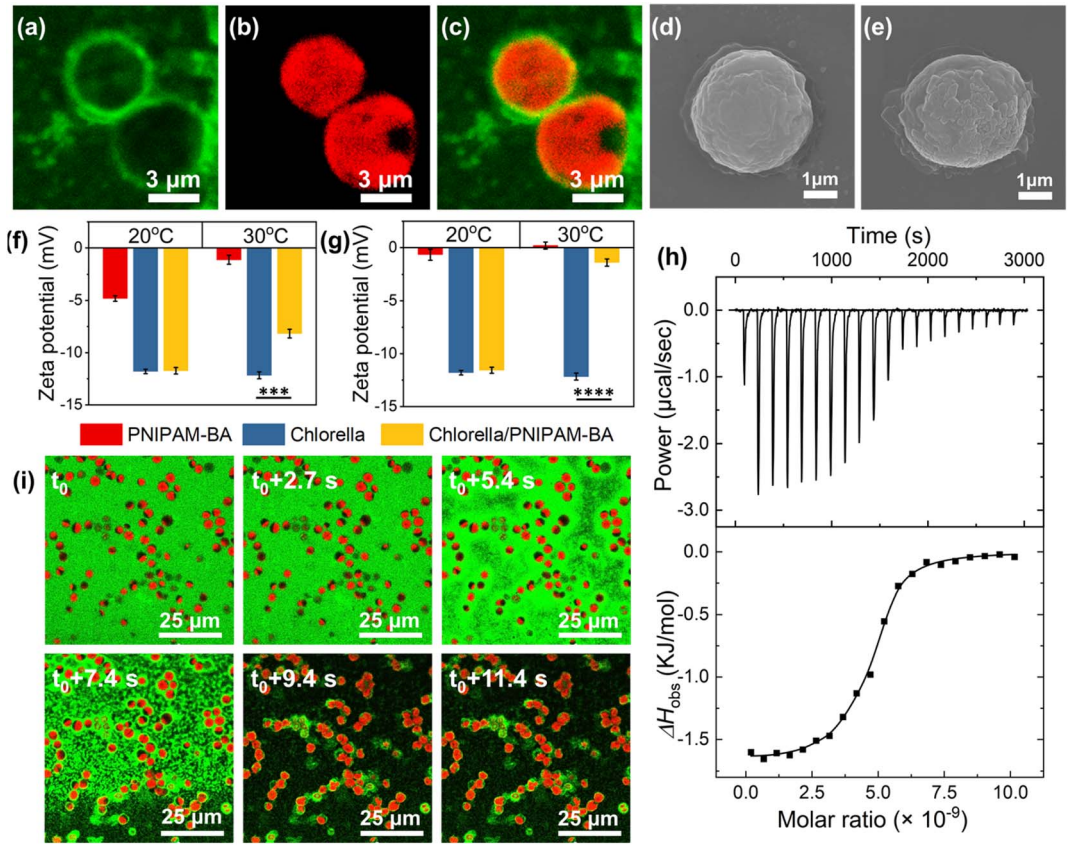

Fig. 2 Interaction mechanism between *Chlorella* and PNIPAM-*co*-BA. CLSM images of *Chlorella*/PNIPAM-*co*-BA complexes with 0.5 wt% PNIPAM-*co*-BA and 7.55×10^7 cells per mL *Chlorella* at 30 °C. (a) The green fluorescence is from the fluorescently labeled PNIPAM-*co*-BA. (b) The red fluorescence is from intracellular chlorophyll. (c) is an overlay of (a) and (b). Scale bars, 3 μm. SEM images of *Chlorella* alone (d) and *Chlorella*/PNIPAM-*co*-BA (e) at 30 °C. Scale bars, 1 μm. Zeta potentials of PNIPAM-*co*-BA, *Chlorella*, *Chlorella*/PNIPAM-*co*-BA at 20 °C and at 30 °C with different PNIPAM-*co*-BA concentrations: ((f) 0.0125 wt%, (g) 0.1 wt%) ($n = 3$, mean ± SD). (h) ITC results of raw and integrated data of released heat for titration of *Chlorella* suspension to PNIPAM-*co*-BA solution at 30 °C. (i) Time-lapse confocal fluorescence images demonstrate the enrichment of PNIPAM-*co*-BA on the surface of *Chlorella* during *in situ* heating. In this study, a low concentration of 0.5 wt% PNIPAM-*co*-BA was specially used to avoid the formation of gel affecting the visualization of the images. Scale bars, 25 μm.

video also demonstrated the uniformly dispersed green fluorescence of PNIPAM-*co*-BA enriched on the surface of *Chlorella* during the heating sol–gel transition of the living material (Video S2† and Fig. 2i). Similarly, SEM images showed that the *Chlorella* in the SSLM also exhibited a clean and smooth surface, while the *Chlorella* in the GSLM exhibited an uneven surface with a large number of copolymer aggregates (Fig. 2d and e). The particle size increased from 2.7 μm to 4.1 μm after *Chlorella* was mixed with PNIPAM-*co*-BA at 30 °C (Fig. S23b†). Moreover, both zeta potential and isothermal titration microcalorimetry (ITC) were employed to investigate the interaction mechanism. At 20 °C, the zeta potential of the *Chlorella* in the living material was almost the same as that of native *Chlorella* (−12.1 mV). At 30 °C, as the copolymer concentration increased, the zeta potential of *Chlorella* in the living materials was significantly lower than that of natural *Chlorella*. This indicates that PNIPAM-*co*-BA did not shield the negatively charged *Chlorella* surface at 20 °C; but at 30 °C, the *Chlorella* exhibited a reduced negative potential due to the shading of the surface by PNIPAM-*co*-BA (Fig. 2f, g and S22†). ITC curves were obtained for the titration of *Chlorella* into PNIPAM-*co*-BA suspensions at 20 °C and 30 °C (Fig. S23a† and 2h, respectively). The titration exothermic enthalpy at 20 °C was almost zero. Thermodynamic data obtained from titration curves at 30 °C indicated that the binding of *Chlorella* to PNIPAM-*co*-BA was mainly entropy-driven, as the change in entropy was positive and the contribution of $-T\Delta S°$ (−9549.23 cal mol^{-1}) to $\Delta G°$ was larger than $\Delta H°$ (−1631.57 ± 36.71 cal mol^{-1}) in magnitude. The cell walls of *Chlorella* are composed of a cellulosic inner wall and an outer hydrophobic algaenan layer.[36,37] PNIPAM-*co*-BA undergoes a phase transition from hydrated coils to dehydrated globules when heated above the LCST.[38] Therefore, the hydrophobic interaction between PNIPAM-*co*-BA and the cell wall of *Chlorella* at 30 °C should mainly contribute to the positive entropy $\Delta S°$, resulting in the self-assembly of SSLM to form GSLM.

Functionality switching of *Chlorella* from photosynthesis oxygen production to hydrogen production

Normally the *Chlorella* cells were loosely distributed in the solution when the living material was in the sol state (Fig. 3a, b, S28 and 29†) and they performed photosynthesis for oxygen

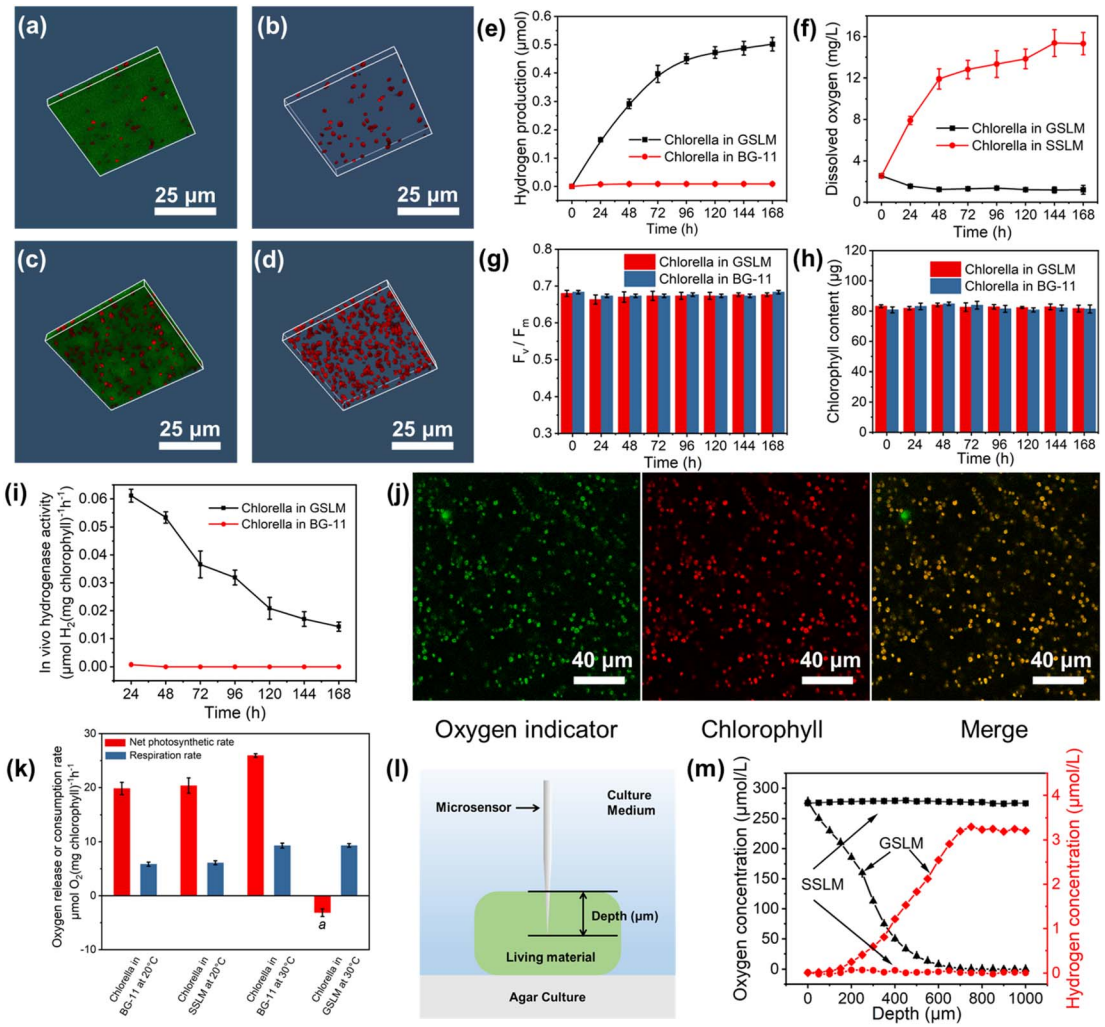

Fig. 3 *Chlorella* produced hydrogen in the GSLM. 3D CLSM images of the SSLM (a and b) and GSLM (c and d). Red fluorescence represents *Chlorella* and green fluorescence represents PNIPAM-*co*-BA labelled by fluorescein *O*-methacrylate. Scale bars, 25 μm. (e) The accumulated amount of hydrogen production from the GSLM (blank squares) and *Chlorella* alone (red circles) at 30 °C in BG-11 solution at different time periods ($n = 3$, mean ± SD). Unless otherwise specified, the volume of *Chlorella* suspension used was 2 mL (7.55×10^7 cells per mL). (f) Dissolved oxygen concentration of the GSLM (black squares) and SSLM (red circles) at 30 °C ($n = 3$, mean ± SD). (g) Maximum quantum yield of PSII (F_V/F_M) of the GSLM (red) and native *Chlorella* cells (blue) at 30 °C ($n = 3$, mean ± SD). We first switched the living material from the gel state to the sol state to release the algae, then centrifuged and dispersed the algae and incubated them in BG-11 medium for 2 hours, and finally used a chlorophyll fluorometer to measure the F_V/F_M of the algae. (h) Total amount of chlorophyll in the GSLM (red) and native *Chlorella* cells (blue) at 30 °C in 2 mL of solution ($n = 3$, mean ± SD). (i) *In vivo* hydrogenase activity in the GSLM (black squares) and native *Chlorella* cells (red circles) at 30 °C ($n = 3$, mean ± SD). (j) The anaerobic state of *Chlorella* in the living material was demonstrated by using an oxygen indicator $[Ru(dpp)_3]Cl_2$ which could generate green fluorescence under anaerobic conditions. The fluorescence of the dye was excited under anaerobic conditions. The green fluorescence was from the oxygen indicator, and the red fluorescence was from intracellular chlorophyll. Scale bars, 40 μm. (k) Net photosynthetic rate (red) and respiration rate (blue) of *Chlorella* in BG-11 at 20 °C, SSLM at 20 °C, BG-11 at 30 °C, and GSLM at 30 °C ($n = 5$, mean ± SD). [a]The net photosynthetic rate was negative, indicating the formation of an anaerobic environment. (l) Schematic illustration showing the microsensor measurement. (m) Hydrogen (red) and oxygen (black) concentrations in the SSLM and GSLM as a function of probe insertion depth ($n = 4$, mean ± SD).

production. Whereas, after forming the GSLM, the crowdedness of the *Chlorella* obviously increased (Fig. 3c, d, S28 and 29†) which would then lead to functionality switching of the *Chlorella* from normal photosynthesis for oxygen production to hydrogen production. We performed experiments in BG-11 medium composed entirely of inorganic salts. As shown in Fig. 3e, no hydrogen production was detected from the *Chlorella* alone in the BG-11 solution, while the formed GSLM could produce hydrogen for 7 days, with an average rate of 0.11 μmol per day for the first four days. We contributed the formation of an anaerobic microenvironment induced by the shrinkage of the polymer matrix to the hydrogen-producing switching mechanism of the constructed living materials. It was observed that with increasing temperature, the living material switched to the gel state, and the volume of the matrix shrank by 9 times (Table S1†), which shortened the distance between the *Chlorella*

and increased the shading effect (Fig. S26 to 30†). As shown in Fig. 3k, negligible differences were observed with PNIPAM-*co*-BA by itself on the respiration rate and photosynthetic rate of the *Chlorella*. The photosynthetic rate subsequently decreased while the respiration rate increased from 5.84 to 9.29 μmol O_2 per mg chlorophyll per h (Fig. 3k), resulting in the formation of an anaerobic microenvironment inside the GSLM accompanied by the activation of hydrogenases (Fig. 3i). The fluorescence of an oxygen indicator $[Ru(dpp)_3]Cl_2$ was quenched under aerobic conditions and excited under anaerobic conditions. As shown in Fig. 3j and S31,† an obvious oxygen indicator signal was detected in the GSLM, while no oxygen indicator signal was detected in the SSLM, which indicated that the *Chlorella* in the GSLM were in an anaerobic state and the *Chlorella* in the SSLM were in an aerobic state. This was also consistent with the reduction of dissolved oxygen concentration from 2.55 to 1.18 mg L^{-1} (Fig. 3f) in GSLM. However, the dissolved oxygen concentration from the SSLM increased from 2.55 to 15.31 mg L^{-1} (Fig. 3f) due to photosynthetic oxygen production, and no hydrogen production was detected (Fig. S32†). Microsensor experiments were performed to examine the hydrogen concentration. In GSLM, the hydrogen concentration increased as the probe insertion depth increased, and it reached a maximum constant value of *ca.* 3.2 μmol L^{-1} at a depth of 700 μm (Fig. 3l and m). In contrast, the oxygen concentration decreased accordingly and was almost zero at a depth of 650 μm in GSLM. A uniform oxygen concentration (*ca.* 277.83 μmol L^{-1}) and nearly zero hydrogen concentration were shown in the SSLM (Fig. 3m).

The continuous supply of electrons from the water oxidation reaction at the PSII reaction center is a key factor affecting sustained photobiological hydrogen production. This is well indicated by a control experiment that showed that with the addition of a PSII inhibitor 3-(3,4-dichlorophenyl)-1,1-dimethylurea (DCMU) to the GSLM, 80% of the hydrogen production was inhibited (Fig. S33†). Moreover, as a light-harvesting molecule, chlorophyll also plays an important role in the operation of the PSII reaction center.[39,40] In this regard, F_V/F_M (the maximal quantum yield of PSII) is a sensitive indicator of the photosynthetic performance of algae, representing the maximum light energy conversion efficiency of PSII.[41] Excitingly, both the algae chlorophyll content and F_V/F_M were negligibly different in the formed GSLM compared with the native *Chlorella*, suggesting that the activity of the *Chlorella* PSII was well maintained (Fig. 3g and h) which then laid the foundation for boosting hydrogen production from the constructed living materials.

To further investigate the hydrogen production mechanism, TAP medium was employed to replace the BG-11 medium, due to the presence of acetic acid (1 mL L^{-1}) in TAP medium which could serve as a respiration substrate for *Chlorella* to favor the formation of an anaerobic environment as well as providing hydrogenase with more electrons to generate hydrogen.[42] When the GSLM was placed into TAP medium, the first 4 days average hydrogen production rate (0.112 μmol H_2 per mg chlorophyll per h) (Fig. 4a and b) was 2.43 times higher than that in BG-11 medium (0.046 μmol H_2 per mg chlorophyll per h) (Fig. 3i). Then the metabolic activities of *Chlorella* after the formation of the GSLM were investigated. When *Chlorella* produced hydrogen in the GSLM for 7 days, the content of light-dependent reaction products—ATP and NADPH—decreased by 39.8% and 38.1% as the content of $NADP^+$ (the oxidized form of NADPH) increased by 53.1% (Fig. S38†), which was mainly due to the influence of the GSLM on the shading effects on core *Chlorella*. There was no significant difference in ATP, NADPH or $NADP^+$ contents of *Chlorella* in the control group (Fig. S39†). Meanwhile, the protein and carbohydrate contents decreased by 21.7% and 68.3%, while the lipid content increased by 31.0% (Fig. 4f–h). We did not observe any significant differences in protein, carbohydrate or lipid contents of *Chlorella* in SSLM or TAP medium (Fig. S40†). Therefore, it could be concluded that both the reduction of NADPH and the catabolic reactions of carbohydrates in the form of starch or glycogen should provide the additional source of endogenous electrons for hydrogen boosting during the dark reaction.[43–45] From day 4 to day 7, the decrease in hydrogen production rate and hydrogenase activity were primarily attributed to the consumption of NADPH and carbohydrates (Fig. S36†).

Temperature-modulated on/off hydrogen production

Although photohydrogen production was accompanied by consumption of the endogenous photosynthesized carbohydrates, the temperature-modulated reversible sol transition of the constructed system could significantly recover the light-dependent reaction products and accumulation of endogenous organic matter (Fig. 4i and j). As observed, after *Chlorella* hydrogen production for 2 days in the GSLM, proliferation of *Chlorella* in SSLM was detected (Fig. 4c). This proliferation then endowed the constructed system with sustainability. In particular, given that the amount of *Chlorella* was closely related to hydrogen production, the proliferation of *Chlorella* would then contribute an exponential enhancement in the amount of hydrogen from the next round of formation of the GSLM. To demonstrate this, we designed experiments in which the *Chlorella* were in the GSLM for 2 days for hydrogen production and 4 days in the SSLM for recovery and proliferation, by repeating 4 cycles (Fig. 4c and d). In each cycle, to keep the *Chlorella* in the same environment, the TAP medium was replaced after the *Chlorella* and copolymer matrix had formed the GSLM. On day 0, day 6, day 12, and day 18, the concentrations of *Chlorella* were 6.13×10^6, 1.82×10^7, 5.89×10^7, and 1.72×10^8 cells per mL, respectively, and as anticipated, the GSLM showed significant *in situ* enhancement in hydrogen production, with rates of 0.11, 0.35, 0.54, and 0.71 μmol per day for 2 days in these four stages, respectively. Since in the fourth gel-state stage, the *Chlorella* concentration was as high as 1.72×10^8 cells per mL, this resulted in *ca.* 20% of *Chlorella* not being able to participate in the formation of the GSLM (Fig. S37†), which then retarded the enhancement in hydrogen production.

Currently, the hydrogen production of algae is primarily regulated by switching the algae between a sulfur-containing medium and a sulfur-deprived medium,[29] or "turning on/off"

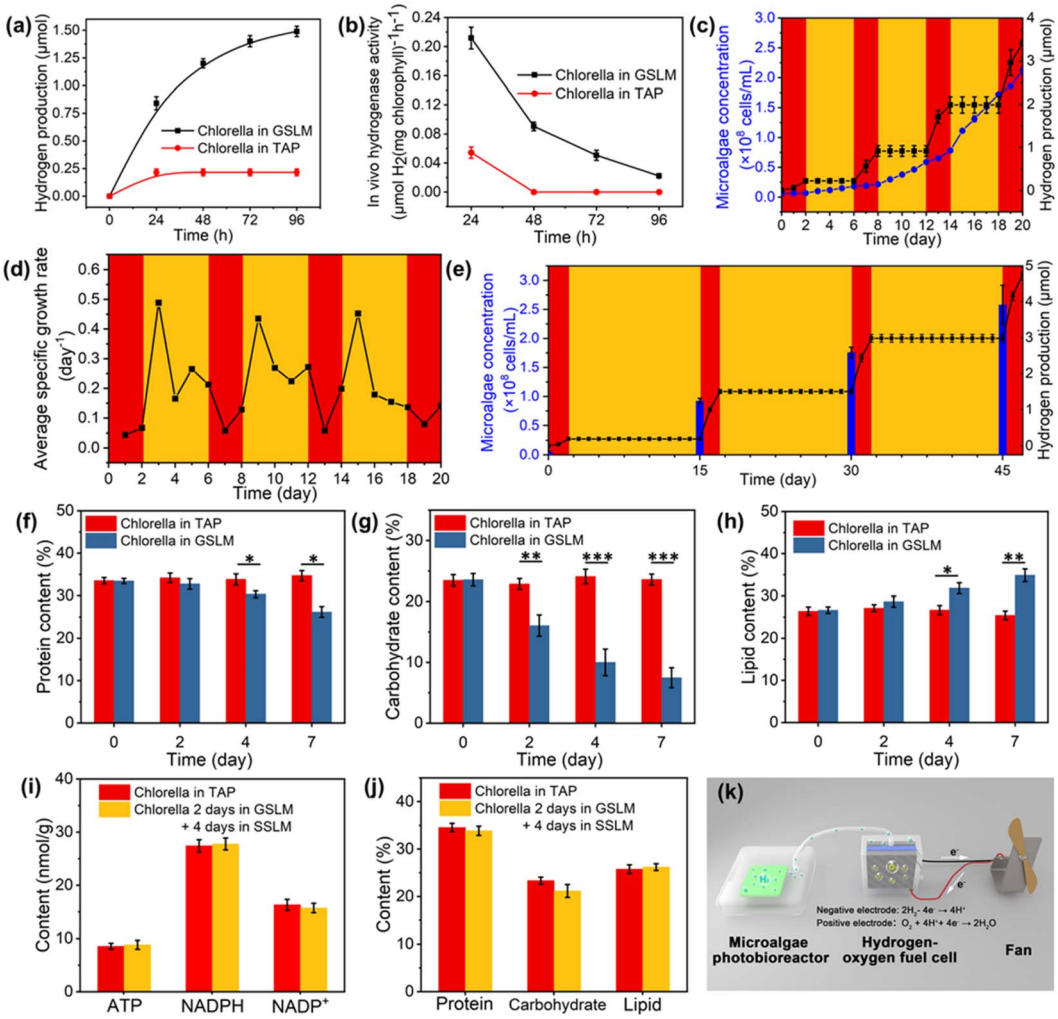

Fig. 4 Regulation of hydrogen production of *Chlorella* in the GSLM. (a) The accumulated amount of hydrogen production from the GSLM (blank squares) and *Chlorella* alone (red circles) at 30 °C in TAP solution at different time periods ($n = 3$, mean ± SD). Unless otherwise specified, the volume of *Chlorella* suspension used was 2 mL (7.55×10^7 cells per mL). (b) *In vivo* hydrogenase activity in the GSLM (black squares) and native *Chlorella* (red circles) at 30 °C in TAP solution ($n = 3$, mean ± SD). For (c)–(e), the red regions represent the GSLM at 30 °C and the yellow regions represent the SSLM at 20 °C. (c) Tunable function of the living material between hydrogen production (black squares) and *Chlorella* proliferation (blue circles) through the transition of the GSLM and SSLM in TAP solution ($n = 3$, mean ± SD). The culture medium was changed every 6 days. Algae concentrations included free algae as well as algae encapsulated in gel. (d) Average specific growth rates of *Chlorella* in the GSLM and SSLM in TAP solution ($n = 3$, mean ± SD). The average specific growth rate of free algae in the SSLM and the average specific growth rate of algae encapsulated in the GSLM were calculated. The culture medium was changed every 15 days. (e) Cumulative H_2 amount and *Chlorella* concentration in sealed tubes during the transition between the GSLM and SSLM in TAP solution ($n = 3$, mean ± SD). The (f) protein, (g) carbohydrate, and (h) lipid contents of *Chlorella* in TAP and GSLM at 30 °C. (i) The contents of ATP, NADPH and $NADP^+$ after *Chlorella* had produced hydrogen in GSLM for 2 days and was cultured in the SSLM for 4 days ($n = 4$, mean ± SD). (j) The contents of protein, carbohydrate and lipid after *Chlorella* had produced hydrogen in the GSLM for 2 days and was cultured in the SSLM for 4 days ($n = 3$, mean ± SD). (k) Schematic diagram of *Chlorella* producing hydrogen to drive a hydrogen fuel cell to rotate a fan (300 mL of *Chlorella* suspension with concentration of 6.51×10^6 cells per mL). The hydrogen produced by the GSLM in the photobioreactor was converted into electricity by a hydrogen–oxygen fuel cell to drive a fan.

gene promoters.[30] Alternatively, by simply controlling the temperature, we could achieve multiple reversible large-scale on/off switching of oxygen and hydrogen evolution, which should be a key step forward in this field. As summarized in Fig. 4c and S41,† when the temperature was below the LCST (20 °C), the constructed system was in the sol state and no hydrogen was produced. By contrast, when the temperature was above the LCST (30 °C), the living material was in the gel state and with the formation of an anaerobic microenvironment hydrogen production was triggered. Excitingly, the survival ratio of *Chlorella* could remain more than 94% after 45 days inside the living material by changing the TAP medium every 15 days (Fig. S42 and S43†). Therefore, for such a constructed living material, we could achieve on-demand hydrogen and oxygen production within 45 days. For example, on day 0, day 15, day 30, and day 45, the concentrations of *Chlorella* were 5.62×10^6, 9.25×10^7, 1.76×10^8 and 2.58×10^8 cells per mL, respectively, with hydrogen

production rates of 0.09, 0.65, 0.74, and 0.89 μmol per day (Fig. 4e). The total amount of chlorophyll increased from 12.96 to 248.64 μg in 2 mL of system. Also, hydrogenase activity was well maintained in the GSLM. In addition, the relative molar mass of PNIPAM–BA was not found to decrease, which indicated that PNIPAM–BA was not decomposed by the algae (Fig. S35†). Compared with other construction methods, the algae-based smart living materials show the same order of average light-to-hydrogen conversion efficiency (0.378‰, in this study) without adding other high-value chemicals, such as glucose,[18] sodium dithionite,[46] enzymes or tannic acid[17] (Table S2†). More importantly, our developed system could continue on-demand oxygen and hydrogen evolution for as long as 45 days, which should be a key breakthrough for the further design of algae-based green energy applications. As a proof-of-concept, we also tried to scale up the constructed system. In this demonstration, we used 5 wt% copolymer and 6.51×10^6 cells per mL *Chlorella* suspension to generate SSLM in 300 mL of algae photobioreactor, and then the *Chlorella* proliferated to 1.73×10^8 cells per mL to form the GSLM. The photobioreactor was placed under a light intensity of 50 $\mu E \cdot m^{-2}\ s^{-1}$ for 4 days, and then about 7 mL of hydrogen was collected from the GSLM, which could be successfully utilized to drive a hydrogen fuel cell to rotate a fan (Fig. 4k, S44 and Video S3†).

Conclusions

In summary, by employing *Chlorella* and PNIPAM-*co*-BA as building blocks, we showed a way to generate a new type of temperature-responsive *Chlorella* cell/polymer hybrid living material for modulating hydrogen boosting. We revealed the functional synergism between the polymer matrix and *Chlorella*, which should be a successful paradigm to actively bridge nonliving matrices and living cells. When the temperature was below the LCST (20 °C), the living material was in the sol state with oxygen production, and by increasing the temperature above the LCST (30 °C), the living material switched to the gel state with hydrogen production. Such a developed *Chlorella* cell/polymer hybrid living material shows excellent biocompatibility, as reflected in the high PSII activity and high survival ratio, as well as proliferation, which then successfully endow the living material with a long-term and high hydrogen production rate. In particular, due to the reversible sol–gel transition of the constructed living material, an on-demand on/off modulation of hydrogen and oxygen evolution of the *Chlorella* within 45 days is achieved. Therefore, given the limited strategies to achieve the reversible on/off modulation of biological hydrogen production, it is anticipated that our studies by integrating a smart polymer matrix and living cells could provide a new method for on-demand functionality modulation of living material for oxygen and hydrogen evolution. Moreover, it is also anticipated that the method described here could represent a prototype strategy for generating multiple functionalized living materials by combining different living cells towards various applications in the fields of biomanufacturing, 3D printing, and environmental bioremediation *etc.*

Data availability

All datasets supporting our findings in this study are available from the corresponding authors upon reasonable request.

Author contributions

The manuscript was written through contributions of all authors. All authors have given approval to the final version of the manuscript.

Conflicts of interest

There are no conflicts to declare.

Acknowledgements

We thank NSFC (22171058), the Fundamental Research Funds for the Central Universities (HIT.OCEF.2023040) and China-German Mobility Programme (M-0470) for financial support.

Notes and references

1 J. M. Lawrence, R. M. Egan, T. Hoefer, A. Scarampi, L. Shang, C. J. Howe and J. Z. Zhang, Rewiring Photosynthetic Electron Transport Chains for Solar Energy Conversion, *Nat. Rev. Bioeng.*, 2023, 1–19, DOI: 10.1038/s44222-023-00093-x.

2 R. E. Blankenship, D. M. Tiede, J. Barber, G. W. Brudvig, G. Fleming, M. Ghirardi, M. R. Gunner, W. Junge, D. M. Kramer, A. Melis, T. A. Moore, C. C. Moser, D. G. Nocera, A. J. Nozik, D. R. Ort, W. W. Parson, R. C. Prince and R. T. Sayre, Comparing Photosynthetic and Photovoltaic Efficiencies and Recognizing the Potential for Improvement, *Science*, 2011, **332**(6031), 805–809.

3 J. E. W. Polle, S.-D. Kanakagiri and A. Melis, Tla1, a DNA Insertional Transformant of the Green Alga Chlamydomonas Reinhardtii with a Truncated Light-Harvesting Chlorophyll Antenna Size, *Planta*, 2003, **217**(1), 49–59.

4 J. Mathews and G. Wang, Metabolic Pathway Engineering for Enhanced Biohydrogen Production, *Int. J. Hydrogen Energy*, 2009, **34**(17), 7404–7416.

5 S. Wu, R. Huang, L. Xu, G. Yan and Q. Wang, Improved Hydrogen Production with Expression of hemH and Lba Genes in Chloroplast of Chlamydomonas Reinhardtii, *J. Biotechnol.*, 2010, **146**(3), 120–125.

6 S. Kosourov, M. Böhm, M. Senger, G. Berggren, K. Stensjö, F. Mamedov, P. Lindblad and Y. Allahverdiyeva, Photosynthetic Hydrogen Production: Novel Protocols, Promising Engineering Approaches and Application of Semi-synthetic Hydrogenases, *Physiol. Plant.*, 2021, **173**(2), 555–567.

7 X. Fang, S. Kalathil and E. Reisner, Semi-Biological Approaches to Solar-to-Chemical Conversion, *Chem. Soc. Rev.*, 2020, **49**(14), 4926–4952.

8 N. Kornienko, J. Z. Zhang, K. K. Sakimoto, P. Yang and E. Reisner, Interfacing Nature's Catalytic Machinery with

Synthetic Materials for Semi-Artificial Photosynthesis, *Nat. Nanotechnol.*, 2018, **13**(10), 890–899.

9 K. Xiao, T. H. Tsang, D. Sun, J. Liang, H. Zhao, Z. Jiang, B. Wang, J. C. Yu and P. K. Wong, Interfacing Iodine-Doped Hydrothermally Carbonized Carbon with Escherichia Coli through an "Add-on" Mode for Enhanced Light-Driven Hydrogen Production, *Adv. Energy Mater.*, 2021, **11**(21), 2100291.

10 M. Martins, C. Toste and I. A. C. Pereira, Enhanced Light-Driven Hydrogen Production by Self-Photosensitized Biohybrid Systems, *Angew. Chem., Int. Ed.*, 2021, **60**(16), 9055–9062.

11 K. Xiao, J. Liang, X. Wang, T. Hou, X. Ren, P. Yin, Z. Ma, C. Zeng, X. Gao, T. Yu, T. Si, B. Wang, C. Zhong, Z. Jiang, C.-S. Lee, J. C. Yu and P. K. Wong, Panoramic Insights into Semi-Artificial Photosynthesis: Origin, Development, and Future Perspective, *Energy Environ. Sci.*, 2022, **15**(2), 529–549.

12 B. Luo, Y.-Z. Wang, D. Li, H. Shen, L.-X. Xu, Z. Fang, Z. Xia, J. Ren, W. Shi and Y.-C. Yong, A Periplasmic Photosensitized Biohybrid System for Solar Hydrogen Production, *Adv. Energy Mater.*, 2021, **11**(19), 2100256.

13 W. Wei, P. Sun, Z. Li, K. Song, W. Su, B. Wang, Y. Liu and J. Zhao, A Surface-Display Biohybrid Approach to Light-Driven Hydrogen Production in Air, *Sci. Adv.*, 2018, **4**(2), eaap9253.

14 L. Shu, W. Xiong, C. Shao, T. Huang, P. Duan, K. Liu, X. Xu, W. Ma and R. Tang, Improvement in the Photobiological Hydrogen Production of Aggregated *Chlorella* by Dimethyl Sulfoxide, *ChemBioChem*, 2018, **19**(7), 669–673.

15 W. Xiong, X. Zhao, G. Zhu, C. Shao, Y. Li, W. Ma, X. Xu and R. Tang, Silicification-Induced Cell Aggregation for the Sustainable Production of H_2 under Aerobic Conditions, *Angew. Chem., Int. Ed.*, 2015, **54**(41), 11961–11965.

16 Z. Xu, S. Wang, C. Zhao, S. Li, X. Liu, L. Wang, M. Li, X. Huang and S. Mann, Photosynthetic Hydrogen Production by Droplet-Based Microbial Micro-Reactors under Aerobic Conditions, *Nat. Commun.*, 2020, **11**(1), 5985, DOI: **10.1038/s41467-020-19823-5**.

17 D. Su, J. Qi, X. Liu, L. Wang, H. Zhang, H. Xie and X. Huang, Enzyme-Modulated Anaerobic Encapsulation of *Chlorella* Cells Allows Switching from O_2 to H_2 Production, *Angew. Chem., Int. Ed.*, 2019, **58**(12), 3992–3995.

18 J. Chen, J. Li, Q. Li, S. Wang, L. Wang, H. Liu and C. Fan, Engineering a Chemoenzymatic Cascade for Sustainable Photobiological Hydrogen Production with Green Algae, *Energy Environ. Sci.*, 2020, **13**(7), 2064–2068.

19 X. Zhu, Z. Xu, H. Tang, L. Nie, R. Nie, R. Wang, X. Liu and X. Huang, Photosynthesis-Mediated Intracellular Biomineralization of Gold Nanoparticles inside Chlorella Cells towards Hydrogen Boosting under Green Light, *Angew. Chem., Int. Ed.*, 2023, **62**(33), e202308437.

20 Z. Xu, J. Qi, S. Wang, X. Liu, M. Li, S. Mann and X. Huang, Algal Cell Bionics as a Step towards Photosynthesis-Independent Hydrogen Production, *Nat. Commun.*, 2023, **14**(1), 1872, DOI: **10.1038/s41467-023-37608-4**.

21 L. M. Utschig, S. R. Soltau, K. L. Mulfort, J. Niklas and O. G. Poluektov, Z-Scheme Solar Water Splitting via Self-Assembly of Photosystem I-Catalyst Hybrids in Thylakoid Membranes, *Chem. Sci.*, 2018, **9**(45), 8504–8512.

22 P. Wang, A. Frank, J. Appel, M. Boehm, N. Strabel, M. M. Nowaczyk, W. Schuhmann, F. Conzuelo and K. Gutekunst, In Vivo Assembly of Photosystem I-Hydrogenase Chimera for In Vitro PhotoH_2 Production, *Adv. Energy Mater.*, 2023, **13**(14), 2203232.

23 N. Rashid, K. Lee, J. Han and M. Gross, Hydrogen Production by Immobilized Chlorella Vulgaris: Optimizing pH, Carbon Source and Light, *Bioprocess Biosyst. Eng.*, 2013, **36**(7), 867–872.

24 L. Gabrielyan, L. Hakobyan and A. Trchounian, Characterization of Light-Dependent Hydrogen Production by New Green Microalga Parachlorella Kessleri in Various Conditions, *J. Photochem. Photobiol., B*, 2017, **175**, 207–210.

25 F. Wang, W.-J. Liang, J.-X. Jian, C.-B. Li, B. Chen, C.-H. Tung and L.-Z. Wu, Exceptional Poly(Acrylic Acid)-Based Artificial [FeFe]-Hydrogenases for Photocatalytic H_2 Production in Water, *Angew. Chem., Int. Ed.*, 2013, **52**(31), 8134–8138.

26 A. Rodrigo-Navarro, S. Sankaran, M. J. Dalby, A. del Campo and M. Salmeron-Sanchez, Engineered Living Biomaterials, *Nat. Rev. Mater.*, 2021, **6**(12), 1175–1190.

27 X. Liu, M. E. Inda, Y. Lai, T. K. Lu and X. Zhao, Engineered Living Hydrogels, *Adv. Mater.*, 2022, **34**(26), 2201326.

28 W. Xiong, Y. Peng, W. Ma, X. Xu, Y. Zhao, J. Wu and R. Tang, Microalgae–Material Hybrid for Enhanced Photosynthetic Energy Conversion: A Promising Path towards Carbon Neutrality, *Natl. Sci. Rev.*, 2023, **10**(10), nwad200.

29 T. Laurinavichene, S. Kosourov, M. Ghirardi, M. Seibert and A. Tsygankov, Prolongation of H2 Photoproduction by Immobilized, Sulfur-Limited Chlamydomonas Reinhardtii Cultures, *J. Biotechnol.*, 2008, **134**(3), 275–277.

30 Y. Wang, X. Jiang, C. Hu, T. Sun, Z. Zeng, X. Cai, H. Li and Z. Hu, Optogenetic Regulation of Artificial microRNA Improves H_2 Production in Green Alga Chlamydomonas Reinhardtii, *Biotechnol. Biofuels*, 2017, **10**(1), 257, DOI: **10.1186/s13068-017-0941-7**.

31 H. Li, Y. Liu, Y. Wang, M. Chen, X. Zhuang, C. Wang, J. Wang and Z. Hu, Improved Photobio-H_2 Production Regulated by Artificial miRNA Targeting psbA in Green Microalga Chlamydomonas Reinhardtii, *Biotechnol. Biofuels*, 2018, **11**(1), 36, DOI: **10.1186/s13068-018-1030-2**.

32 S. Wang, Z. Xu, S. Lin, X. Liu, L. Wang and X. Huang, Polymer-Chlorella Cells Conjugating with Aggregation-Induced Functionality Switch towards Hydrogen Evolution, *Sci. China: Technol. Sci.*, 2020, **63**(8), 1416–1425.

33 J. Chen, Y. Li, M. Li, J. Shi, L. Wang, S. Luo and H. Liu, Chemical Flocculation-Based Green Algae Materials for Photobiological Hydrogen Production, *ACS Appl. Bio Mater.*, 2022, **5**(2), 897–903.

34 S. Weber, P. M. Grande, L. M. Blank and H. Klose, Insights into cell wall disintegration of Chlorella vulgaris, *PLoS One*, 2022, **17**(1), e0262500, DOI: **10.1371/journal.pone.0262500**.

35 J. Zhang, N. Hori and A. Takemura, Optimization of Preparation Process to Produce Polyurethane Foam Made by Oilseed Rape Straw Based Polyol, *Polym. Degrad. Stab.*, 2019, **166**, 31–39.

36 K. Jothibasu, I. Muniraj, T. Jayakumar, B. Ray, D. W. Dhar, S. Karthikeyan and S. Rakesh, Impact of Microalgal Cell Wall Biology on Downstream Processing and Nutrient Removal for Fuels and Value-Added Products, *Biochem. Eng. J.*, 2022, **187**, 108642.
37 X. Zhou, Y. Zeng, Y. Tang, Y. Huang, F. Lv, L. Liu and S. Wang, Artificial Regulation of State Transition for Augmenting Plant Photosynthesis Using Synthetic Light-Harvesting Polymer Materials, *Sci. Adv.*, 2020, **6**(35), eabc5237.
38 Y. Cai, F. Liu, X. Ma, X. Yang and H. Zhao, Hydrophobic Interaction-Induced Coassembly of Homopolymers and Proteins, *Langmuir*, 2019, **35**(33), 10958–10964.
39 F. Rappaport and B. A. Diner, Primary Photochemistry and Energetics Leading to the Oxidation of the $(Mn)_4Ca$ Cluster and to the Evolution of Molecular Oxygen in Photosystem II, *Coord. Chem. Rev.*, 2008, **252**(3), 259–272.
40 T. K. Antal, T. E. Krendeleva and E. Tyystjärvi, Multiple Regulatory Mechanisms in the Chloroplast of Green Algae: Relation to Hydrogen Production, *Photosynth. Res.*, 2015, **125**(3), 357–381.
41 E. Touloupakis, C. Faraloni, A. M. Silva Benavides, J. Masojídek and G. Torzillo, Sustained photobiological hydrogen production by Chlorella vulgaris without nutrient starvation, *Int. J. Hydrogen Energy*, 2021, **46**(5), 3684–3694.
42 S. R. Vargas, M. Zaiat and M. d. C. Calijuri, Chlamydomonas Strains Respond Differently to Photoproduction of Hydrogen and By-Products and Nutrient Uptake in Sulfur-Deprived Cultures, *J. Environ. Chem. Eng.*, 2021, **9**(5), 105930.
43 E. Shastik, L. Li, L. Zhang, R. Qin, W. Yu and J. Liu, Some Molecular Aspects of Hydrogen Production by Marine Chlorella Pyrenoidosa under Nitrogen Deprivation Condition in Natural Seawater, *Int. J. Hydrogen Energy*, 2020, **45**(27), 13876–13883.
44 A. Melis and T. Happe, Hydrogen Production. Green Algae as a Source of Energy, *Plant Physiol.*, 2001, **127**(3), 740–748.
45 N. Chinchusak, A. Incharoensakdi and S. Phunpruch, Enhancement of Dark Fermentative Hydrogen Production in Nitrogen-Deprived Halotolerant Unicellular Cyanobacterium Aphanothece Halophytica by Treatment with Reducing Agents, *Biomass Bioenergy*, 2022, **167**, 106624.
46 J. He, L. Xi, X. Sun, B. Ge, D. Liu, Z. Han, X. Pu and F. Huang, Enhanced Hydrogen Production through Co-Cultivation of Chlamydomonas Reinhardtii CC-503 and a Facultative Autotrophic Sulfide-Oxidizing Bacterium under Sulfurated Conditions, *Int. J. Hydrogen Energy*, 2018, **43**(32), 15005–15013.